IEEE Access
Multidisciplinary | Rapid Review | Open Access Journal

Received 5 June 2025, accepted 10 July 2025, date of publication 28 July 2025, date of current version 12 August 2025.

Digital Object Identifier 10.1109/ACCESS.2025.3593044

RESEARCH ARTICLE

Grid Integration of PV Systems With Advanced Control and Machine Learning Strategies

VENKATA REDDY KOTA[1], (Senior Member, IEEE), BAPAYYA NAIDU KOMMULA[2], (Member, IEEE), ASIF AFZAL[3,4], (Member, IEEE), MOHAMMAD ASIF[5], (Member, IEEE), AND LIEW TZE HUI[6,7], (Member, IEEE)

[1]Department of Electrical and Electronics Engineering, Jawaharlal Nehru Technological University, Kakinada 533003, India
[2]Department of Electrical and Electronics Engineering, Aditya University, Surampalem, Andhra Pradesh 533437, India
[3]Department of Engineering, University of Luxembourg, 4364 Esch-sur-Alzette, Luxembourg
[4]University Centre for Research and Development, Department of Computer Science and Engineering, Chandigarh University, Mohali, Punjab 140413, India
[5]Department of Chemical Engineering, King Saud University, Riyadh 11421, Saudi Arabia
[6]Centre for Intelligent Cloud Computing (CICC), COE of Advanced, Multimedia University, Melaka 75450, Malaysia
[7]Faculty of Information Science and Technology, Multimedia University, Melaka 75450, Malaysia

Corresponding authors: Liew Tze Hui (thliew@mmu.edu.my) and Bapayya Naidu Kommula (kbapayanaaiidu@gmail.com)

The author from King Saud University acknowledge the financial support from the Ongoing Research Funding Program (ORF-2025-42), King Saud University, Riyadh, Saudi Arabia.

ABSTRACT In the pursuit of sustainable and efficient energy solutions, Photovoltaic (PV) systems have emerged as a prominent player in the domain of renewable energy generation. Particularly, grid-tied PV systems have gained substantial attention due to their potential to contribute to stability and reliability of existing power grid infrastructure. Accordingly, an innovative approach to enhance grid supply using PV systems with Machine Learning Strategy is proposed in this research. The primary objective is to optimize voltage output from PV system while concurrently maximizing power using a novel Modified Zeta-Cuk converter, coupled with Hybrid Maximum Power Point Tracking (MPPT) algorithm combining Incremental Conductance and Bat Optimization Algorithm (InC-BOA). The stabilized DC link resulting from this process is directed to a 3-phase Voltage Source Inverter (VSI) to facilitate conversion of DC supply to AC. To further improve the efficiency and accuracy of system, current produced by inverter is subjected to Discrete Wavelet Transform (DWT) analysis followed by Principal Component Analysis (PCA) for feature extraction. The final step involves implementation of Recurrent Neural Network (RNN) controller, enabling the generation of a refined reference current. The generated reference current is then compared with actual current using Hysteresis Current Controller (HCC). This comparison yields an output which is subsequently employed to Pulse Width Modulation (PWM) generator facilitating the achievement of effective grid synchronization, enhancing overall performance and stability of the system. The validation is performed using MATLAB Simulink software and the outcomes reveals the dominance of proposed work.

INDEX TERMS PV system, InC-BOA MPPT algorithm, modified zeta-cuk converter, machine learning, DWT, PCA, RNN controller, HCC.

I. INTRODUCTION

In recent years, the global community's increasing concern about environmental sustainability and the imperative to address climate change have driven a significant shift towards embracing RESs [1], [2]. In this scenario, PV systems have taken center stage as a highly promising technology for harnessing the sun's abundant energy. PV systems directly convert sunlight into electricity, making them a key component in transition towards cleaner and more sustainable energy generation [3], [4], [5]. Among various PV system configurations, grid-tied PV systems have gained substantial attention due to their potential to revolutionize energy production and distribution [6]. These systems are designed to be flawlessly integrated into existing power grid infrastructure, enabling them to not only generate clean energy but also

The associate editor coordinating the review of this manuscript and approving it for publication was Inam Nutkani.

contribute to the stability and reliability of overall grid [7], [8]. In response to this pressing need, this research introduces an innovative approach that leverages advanced control strategies and state-of-the-art machine learning techniques to optimize the performance of grid-tied PV systems.

To achieve overarching objective of optimizing the performance of grid-tied photovoltaic PV systems, power electronic converter [9] serves as a pivotal element designed to enhance energy conversion efficiency and ensure seamless integration of PV systems with existing power grid infrastructure. Conventional DC-DC [10], [11], [12] converters suffer from limited voltage range, inefficiency at light loads, switching losses and reliability while lacking adaptability to varying conditions. As a result, modified converters are developed to address the limitations of conventional converters and to improve specific aspects of their performance. In [13] modified Buck-Boost converter is proposed, which maintains both voltage step/down process. However, additional stages is required to achieve quadratic Buck-Boost voltage transformation. The interleaved Landsman converter of [14] improves power quality with reduced current ripple and harmonics. Nevertheless, it include increased complexity from interleaving and potential limitations for high-power applications. In [15] modified Single-Ended Primary-Inductor Converter (SEPIC) topology is addressed. Besides its improved efficiency is less suitable for applications characterized by dynamic or unpredictable operating environments. The paper [16] utilizes bidirectional SEPIC-Zeta converter for microgrids to offer seamless power flow. However, demerits such as component stress, efficiency loss and complex control makes the topology failure for high power applications. In contrast to conventional power converters, which often exhibit limitations in accommodating dynamic operational conditions, a novel Modified Zeta-Cuk converter is proposed for PV voltage enhancement.

In the realm of RES, the quest to extract optimal energy yield from PV is a crucial which is achieved by the process of MPPT. Classical MPPT techniques, such as Perturb and Observe (P&O) [17] and InC [18], Fractional Open Circuit Voltage (FOCV) [19], Hill climbing [20] etc. while effective in tracking MPP, exhibit drawbacks like oscillations around optimal point and sensitivity to changing atmospheric conditions. Currently, researchers have directed their attention towards employing soft computing and evolutionary MPPT techniques which are suitable for optimizing nonlinear behavior inherent in PV systems. Several soft computing and biological algorithms, including Artificial Neural Network (NN) [21], Fuzzy Logic Controller (FLC) [22], Adaptive Neuro Fuzzy Interface System (ANFIS) [23], cuckoo search [24], and Particle Swarm Optimization (PSO) [25], have been integrated into evolutionary algorithms for enhanced MPPT. Despite their advantages, evolutionary algorithms exhibit slower convergence rates compared to classical methods in some scenarios, resulting in longer tracking times and potential performance delays. These limitations hinder precise power extraction and overall system stability. To overcome these shortcomings, hybrid MPPT algorithm combining InC-BOA is proposed.

Generating a reference current is essential for aligning the power system with specific grid standards. It begins with a two-step analysis of inverter-generated current: DWT for frequency dissection [26], followed by PCA for feature extraction [27]. The next phase involves RNN controller, capable of capturing intricate temporal patterns, enabling the creation of a sophisticated reference current that harmonizes with grid complexities. Existing converters and techniques lack comprehensive integration of advanced signal processing and machine learning methods, leaving emphasis for enhanced precision and efficiency in photovoltaic systems. This gap permits investigation into practical implementation and validation of proposed framework for advancements and real-world performance. The primary contribution of the work includes:

- Implementation of novel Modified Zeta-Cuk converter with Hybrid InC-BOA to simultaneously optimize voltage output and maximize power generation from the PV system.
- Accomplishment of improved current signal performance by applying DWT analysis for preprocessing and PCA for feature extraction.
- Implementation of RNN controller for refined reference current generation, which enhances grid synchronization, system stability, and overall operation.
- Demonstrating the proposed methodology's effectiveness through validation using MATLAB Simulink software.

A. NOVELTY AND METHODOLOGY

Novelties:

a) To propose a novel approach for enhancing grid supply using PV systems with Machine Learning Strategy.
b) A maiden effort was made to utilize Modified Zeta-Cuk converter for controlling the voltage output from PV systems.
c) To recommend novel a Hybrid Maximum Power Point Tracking (MPPT) algorithm combining Incremental Conductance and Bat Optimization Algorithm (InC-BOA), for maximizing the power output from PV systems.
d) A new control strategy using Discrete Wavelet Transform (DWT) analysis, Principal Component Analysis (PCA) for feature extraction, and Recurrent Neural Network (RNN) controller for grid-tied PV systems is suggested for effective grid synchronization.
e) To develop an experimental prototype of grid connected solar PV with hybrid InC-BOA technique considering DWT, PCA and RNN approaches

Methodologies:

a) To optimize the PV output voltage using a novel modified Zeta-Cuk Converter considering Hybrid MPPT with InC-BOA

b) Real Time validation of the proposed system

The paper is structured by description of proposed framework in Section II, followed by modelling of system components in section III, outcomes of proposed system is described Section IV and finally, Section V encapsulates the research with a comprehensive conclusion of the study's findings and contributions.

II. PROPOSED SYSTEM DESCRIPTION

The proposed research introduces an innovative and comprehensive approach to enhance the efficiency, stability, and performance of grid-tied PV systems through a series of advanced technologies and strategies. Figure 1 illustrates the architecture of proposed framework. The proposed research not only maximizes the power output of PV systems but also ensures their smooth operation within the larger grid network.

The methodology begins with the utilization of a Modified Zeta-Cuk converter, which optimizes the voltage output of PV systems. To further enhance power generation, a unique MPPT algorithm is employed, which intelligently adjusts the converter's parameters based on a combination of InC-BOA techniques. This integrated approach ensures PV system operates at its maximum power point. The stabilized DC output from the converter is then channeled to 3Φ VSI, which serves as intermediary between PV system's DC output and AC grid. This conversion is essential for efficient energy transfer and integration into larger power network. To enhance AC current from inverter, DWT analysis is employed, which separates the current signal into its inherent frequency components. Subsequently, PCA is employed to manage the complexity of frequency components, while reduces the dimensionality of data and retaining critical information. For refined control and accuracy, RNN controller is introduced, that learns intricate patterns from the data and generates a precise reference current profile. The HCC then compares the actual inverter current with the refined reference current. Based on this comparison, PWM generator produces an output signal that fine-tunes the width of signal pulses, effectively controlling the inverter's current output. The PWM-modulated current ensures seamless synchronization with the grid's frequency and phase, enabling smooth integration into the existing power infrastructure.

III. MODELLING OF SYSTEM COMPONENTS

A. DESIGN OF PV SYSTEM

The proposed work utilizes PV as primary source for generating power. Figure 2 illustrates the single diode model of photovoltaic system. The setup of a PV solar system consists of several solar cells that are interconnected using a combination of series and parallel connections to achieve desired output voltage.

According to semiconductor theory, the fundamental mathematical equation governing the current-voltage (I-V) characteristics of a PV cell is expressed as:

$$F(s) = \frac{K_{T_i}}{1/s^{n_i}} + \frac{K_{I_i}}{s} + K_{D_i} s \left(\frac{N_i}{s + N_i} \right)$$
$$I = I_{ph} - I_o \left[e^{\frac{(V+IR_s)}{aN_S KT} q} - 1 \right] - \frac{V + IR_s}{R_{sh}} \quad (1)$$

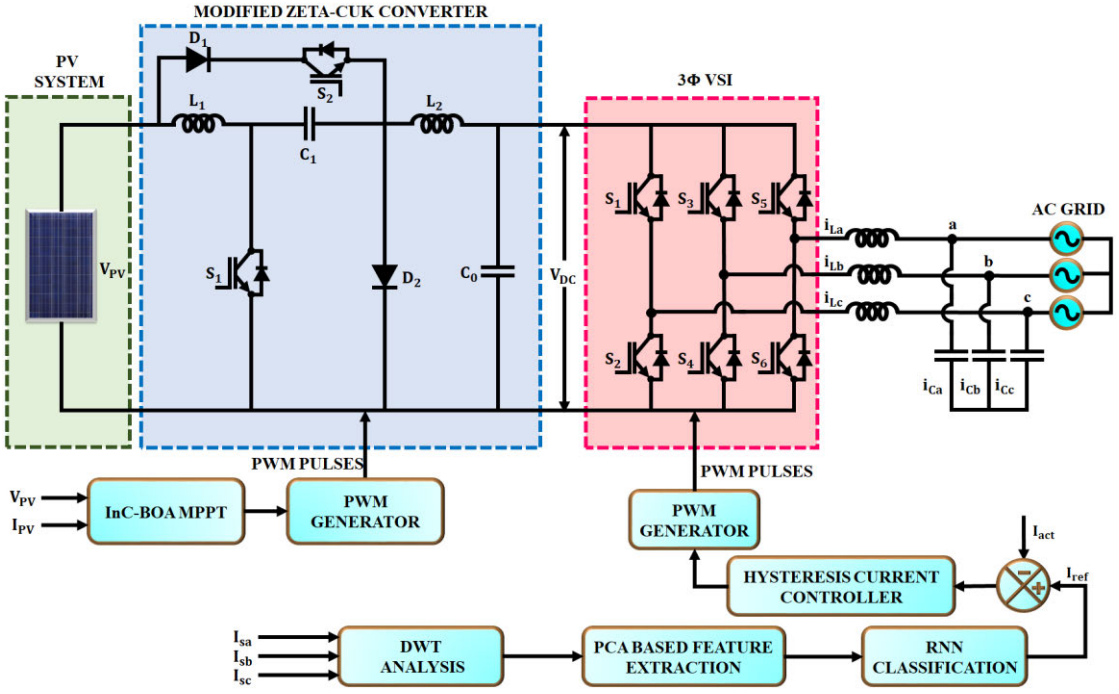

FIGURE 1. Block diagram of proposed ML assisted PV driven grid system.

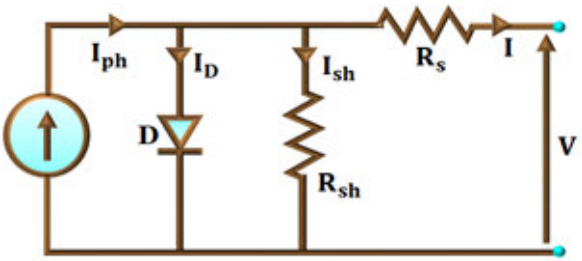

FIGURE 2. PV system configuration.

From equation (1), saturation current of diode and generated photocurrent is specified as I_o and I_{ph}, similarly, the resistance connected in shunt and series is determined as R_{sh} and R_s. Moreover, diode ideality factor is specified as a, number of PV cells connected in series is N_S, electron charge as q, temperature as T and Boltzmann constant as K. Additionally, converter operation is essential to boost the PV voltage, which is described in the subsequent section.

B. OPERATION OF MODIFIED ZETA-CUK CONVERTER

The proposed modified Zeta-Cuk converter depicted in Figure 3, operates in continuous conduction mode to facilitate efficient energy conversion. It combines the characteristics of both Zeta and Cuk converters, enabling continuous voltage regulation and energy transfer.

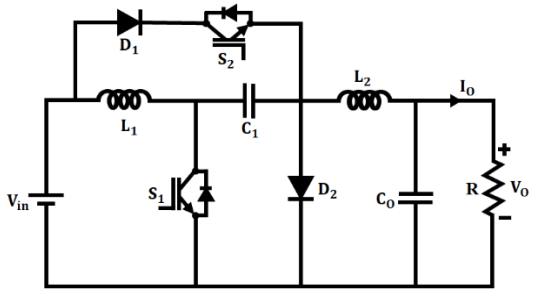

FIGURE 3. Equivalent circuit of modified Zeta-cuk converter.

1) OPERATION AT MODE-I

During the time interval from t_1 to t_2 switch S_1 is in conducting state, while switch S_2 remains off. At this point, the voltage across inductor L_1 matches input voltage V_{in}. The charging process occurs inductively, with L_1 receives input voltage V_{in}, and inductor L_2 being charged via $V_{in} + V_{C1}$. Simultaneously, capacitor C_1 is discharged through inductor L· and output voltage, V_o as illustrated in Figure 4(a).

$$V_{L1} = V_{c1} \tag{2}$$

$$V_{L2} = V_{in} + V_{ca} - V_o \tag{3}$$

2) OPERATION AT MODE-II

In the time interval from t_1 to t_2, switch S_2 is in conducting state while switch S_1 remains in OFF state. This configuration is complemented by the activation of diodes D_1 and D_2. During this period, inductor L_1 discharges its stored energy through capacitor C_1, facilitating energy transfer. Concomitantly, inductor L_2 is charged using input voltage V_{in}. Furthermore, capacitor C_1 experiences charging through the energy transferred from inductor L_1. This dynamic interplay of switches, diodes, and inductors leads to complex energy exchange process illustrated in Figure 4(b).

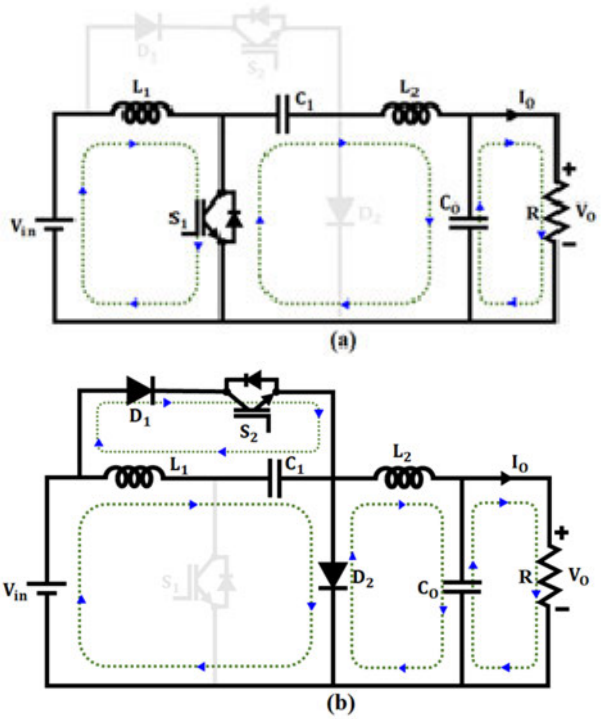

FIGURE 4. Operation of modified Zeta-Cuk converter at (a) Mode-I and (b) Mode-II.

The mathematical expression governing the behavior of these inductors is expressed by

$$V_{L1} = -V_{c1} \tag{4}$$

$$V_{L2} = V_{in} - V_o \tag{5}$$

Applying volt-second balance equation to inductor L_1 results in the determination of capacitor voltage V_{C1}.

$$\frac{1}{T}\left(\int_0^{DT} V_{in}dt + \int_{DT}^{T} V_{c1}dt\right) = 0 \tag{6}$$

By simplifying Equation (6), it becomes feasible to ascertain the average value of V_{C1} as

$$\frac{DV_{in}}{(1-D)} = V_{c1} \tag{7}$$

Utilizing a volt-second balance equation for inductor L_2, the subsequent voltage gain can be derived:

$$\frac{1}{T}\left(\int_0^{DT} (V_{in} + V_{c1} - V_o)\,dt + \int_{DT}^{T} (V_{in} - V_o)\,dt\right) = 0 \tag{8}$$

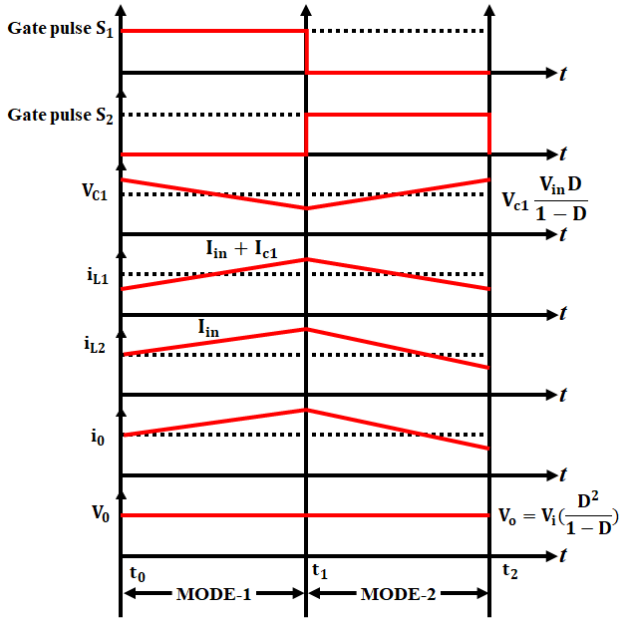

FIGURE 5. Switching cycle of modified Zeta-Cuk converter.

Upon simplifying Equation (8), voltage gain is computed as:

$$\frac{V_o}{V_{in}} = \frac{D^2}{(1-D)} \tag{9}$$

By intelligently switching between these modes, the modified Zeta-Cuk converter optimizes energy conversion and accommodates varying voltage requirements efficiently.

IV. MPPT TECHNIQUE FOR PV SYSTEM

The InC with Bat Optimization Algorithm is an advanced MPPT controller designed to optimize the energy extraction from PV systems under varying environmental conditions. This hybrid approach combines InC algorithm and BOA, leveraging their respective strengths to enhance the efficiency and accuracy of MPPT process.

A. INCREMENTAL CONDUCTANCE (INC) TECHNIQUE

The InC algorithm operates based on the rate of change of power with respect to changes in voltage and current. It calculates the conductance of PV system and compares it with incremental conductance (dP/dV), which is proportional to the power change with respect to voltage change. By adjusting the operating voltage and tracking changes in conductance, InC algorithm seeks to maintain the system at point where power change is zero, indicating that the operating point is close to MPP.

$$\frac{dP}{dV} = 0 \tag{10}$$

The above expression is written as,

$$\frac{dP}{dV} = \frac{d(IV)}{dV} = 1 + V\frac{dI}{dV} = 0 \tag{11}$$

$$\frac{dI}{dV} < -\frac{1}{V} \text{at right of MPP} \tag{12}$$

$$\frac{dI}{dV} > -\frac{1}{V} \text{at left of MPP} \tag{13}$$

$$\frac{dI}{dV} = -\frac{1}{V} \text{at MPP} \tag{14}$$

InC's ability to respond swiftly to changes in solar irradiance and temperature makes it an essential tool in achieving efficient energy conversion. However, its reactivity causes oscillations around MPP, especially in dynamic environments. This limitation has paved the way for exploration of hybrid approaches that complement InC's strengths with global optimization techniques to ensure stable and accurate MPP tracking.

B. BAT OPTIMIZATION ALGORITHM

The Bat algorithm is a nature-inspired optimization technique that mimics the behavior of bats to solve complex optimization problems. In nature, bats use echolocation and adaptive foraging behaviors to locate prey. Similarly, bat algorithm models bats' searching and foraging behaviors to find the optimal solution. Based on feedback intensity, proximity is determined. Higher intensity signifies closeness, prompting the bat to intensify pulse emission for capture. Bats' flight features include random velocity (V_i), position (X_i), and loudness (l_i). Emission rate, within [0, 1] depends on target distance. Bat's velocity and position are updated as follows:

$$X_i^{t+1} = X_i^t + V_i^{t+1} \tag{15}$$

$$X_i^{t+1} = V_i^t + (X_i^t - X^*)f_i \tag{16}$$

The frequency assigned at random is specified as f_i.

$$f_i = f_{min} + (f_{max} - f_{min})\,\varphi \tag{17}$$

where φ is a uniform random variable in [0,1], while x^* is the best global position. During position updates, emission rate influences. If φ surpasses emission, exploitation mode activates. Current position changes using local search solution, given by:

$$X_n = X^* + l^t \tag{18}$$

The random number is drawn from Gaussian or uniform distribution in $[-1, 1]$, while l^t stands for average loudness at that time. The fitness function improves when generated random number is smaller than loudness. Exploration yields a new solution, updating parameters like emission rates and loudness. Mathematically, parameter update is expressed as:

$$l_l^{t+1} = \rho l_l^t \tag{19}$$

$$r_l^{t+1} = r_i(1 - e^{\alpha t}) \tag{20}$$

Here, ρ is a constant ranging from 0 to 1, and $\boldsymbol{\alpha}$ is a positive constant. The behavior simulates a bat's search for food, involving energy tracking to achieve P_{max}point in PV model.

C. PROPOSED HYBRID INC-BOA MPPT TECHNIQUE FOR TRACKING PV POWER

The proposed hybrid InC-BOA approach combines InC's rapid response with bat's optimization capabilities to achieve efficient and stable tracking of solar PV power and the MPP.

1) INITIAL TRACKING WITH InC

At the initial stage of process, InC algorithm is engaged as primary tracker. It responds quickly to changes in solar irradiance and rapidly adjusts the PV system's operating point to track MPP. However, under certain conditions, IncCond exhibit oscillations around MPP due to its reactive nature.

2) BOA AS A FINE-TUNER

This is where BOA comes into performance. When InC encounters oscillations, BOA steps in to fine-tune the tracking process. BOA optimizes the PV system's operating point by considering both local and global best solutions, allowing it to overcome oscillation issue and converge to a stable MPP. BOA introduces global optimization capabilities for tracking process. It guides the system towards true MPP by exploring solution space intelligently. By adjusting the operating point using BOA's equations, the system efficiently finds optimal conditions for power extraction.

Steps in Hybrid Algorithm

Step 1: Initialize bat population with random positions and velocities.

Step 2: Calculate incremental conductance (dI/dV)

Step 3: Determine the direction of voltage change based on the sign of dI/dV.

Step 4: Adjust the voltage based on direction of change and update power output.

Step 5: Evaluate power output and select best solution among the bats.

Step 6: Update bat positions using the BOA equation (20), considering current and global best solutions.

$$\begin{aligned}&\text{NewPosition}\\&= \text{Current Position}\\&\quad + \xi^{*}(\text{Current Position} - \text{Best Position})\\&\quad + \text{A}^{*}(\text{Global Best Position} - \text{Current Position})\\&\quad + \text{rand}()^{*}(\text{Upper Bound} - \text{Lower Bound})\end{aligned} \tag{21}$$

If convergence criteria met

Exit

Else

Step 7: Repeat steps 2 to 6 iteratively.

Step 8: Track the MPP using InC but introduce BOA based adjustment for fine-tuning.

These advanced strategies leverage the adaptability and learning capabilities of optimization algorithms to enhance tracking accuracy, minimize oscillations, and achieve higher efficiency, ensuring optimal power extraction from photovoltaic systems across varying operational conditions.

V. DWT ANALYSIS

DWT is a signal processing technique used for analyzing signals in both time and frequency domains. It decomposes a signal into different frequency components, revealing both high-frequency details and low-frequency trends. In the proposed work DWT is used to analyze the current signal produced by inverter.

A. DWT PROCESS FOR CURRENT SIGNAL ANALYSIS

The process begins by sending signal through a half-band low-pass filter with impulse response h[n]. This filtering is similar to convolving the signal with filter's impulse response. Convolution in discrete time is mathematically defined as:

$$\text{x[n]}^{*}\text{h[n]} = \sum_{k=-\infty}^{\infty} \text{x[n].h[n-k]} \tag{22}$$

A half-band low-pass filter eliminates frequencies above half the signal's maximum frequency. Down sampling output by two discards half the samples without losing information. DWT coefficients contain information from adjacent data, preserving the scale. Low-pass filtering reduces resolution but maintains scale. Subsampling by two removes redundant samples, effectively doubling the scale.

Mathematically, the procedure is expressed by,

$$\text{y[n]} = \sum_{\text{k}=-\infty}^{\infty} \text{h[k].x[2n-k]} \tag{23}$$

The expression for approximate and detailed components is determined as:

$$\text{y}_{\text{hiah}} = \sum\nolimits_{\text{n}} \text{x[n].g[2k-n]} \tag{24}$$

$$\text{y}_{\text{low}}\text{[k]} = \sum\nolimits_{\text{n}} \text{x[n].h[2k-n]} \tag{25}$$

This iterative process yields multiple levels of coefficients, revealing insights into the signal's behavior across various frequency ranges. After preprocessing, feature extraction is performed to extract relevant features from the transformed signal.

VI. PRINCIPAL COMPONENT ANALYSIS FOR FEATURE EXTRACTION

PCA aims to reduce the dimensionality of signal while retaining most relevant information. The DWT-decomposed current signal generates a set of coefficients, which is potentially of high dimension. Applying PCA allows for identification of principal components or directions of maximum variance in this coefficient space. The method necessitates training with diverse data sets representing different testing conditions. To derive Eigen signals, each observation's data set is transformed into a column vector Γ_n with a length of N variables. For M observations, the resulting matrix Γ has dimensions M x N. Thus,

$$\Gamma = [\Gamma_1, \Gamma_2, \Gamma_3, \ldots, \Gamma_{\text{n}}] \tag{26}$$

Average signal ψ is expressed as

$$\psi = \frac{1}{\mathrm{M}} \sum_{n=1}^{\mathrm{M}} \Gamma_{\mathrm{n}} \tag{27}$$

Difference signals are generated by subtracting the mean signal from each training signal:

$$\phi_i = \Gamma_i - \psi \tag{28}$$

These vectors undergo PCA to determine orthogonal eigenvectors. Calculating the covariance matrix C is essential for this process.

$$\mathrm{C} = \frac{1}{\mathrm{M}} \sum_{\mathrm{n}=1}^{\mathrm{M}} \phi_{\mathrm{n}}, \mathrm{C} = \frac{1}{\mathrm{M}} \sum_{\mathrm{n}=1}^{\mathrm{M}} \phi_{\mathrm{n}}$$
$$C = \frac{1}{M} \sum\nolimits_{n=1}^{M} \Phi_n \Phi_n^T = \frac{1}{\mathrm{M}} A \cdot A^T \tag{29}$$

From expression above, $A = [\phi_1, \phi_2, \phi_3, .., \phi_n]$. However, computing eigenvectors for covariance matrix C becomes computationally intensive due to its size N x N. A more efficient alternative is considered, where $\mathrm{V_i}$represents eigenvectors of A x $\mathrm{A^T}$, and corresponding eigenvalues are denoted by:

$$\mathrm{A^T A v_i} = \mu_{\mathrm{i}} \mathrm{v_i} \tag{30}$$

Henceforth, C becomes

$$\mu_{\mathrm{i}} = \mathrm{A v_i} \tag{31}$$

where C = A x $\mathrm{A^T}$. The eigenvectors, referred to as Eigen signals μ_i, are obtained. Among them, top M Eigen signals are selected based on their corresponding largest eigenvalues. Any signal is represented as a linear combination of these Eigen signals. For a signal Γ, its principal components are defined as follows:

$$\mathrm{W_k} = \mu_{\mathrm{k}}^{\mathrm{T}} (\Gamma - \psi) \tag{32}$$

The value W_k represents data anticipated onto the axis associated with eigenvector. These values serve as new features suitable for classification and recognition tasks.

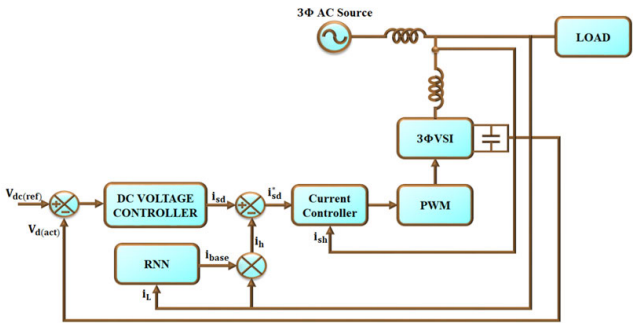

FIGURE 6. RNN based reference current generation.

VII. GENERATION OF REFERENCE CURRENT BY RNN

Harmonics arise from non-linear loads, but methods to mitigate them exist. A powerful strategy involves injecting counteractive harmonics at the Point of Common Coupling (PCC). This demands accurate reference current generation is achieved using RNN.

RNN's architecture resembles an Elman network, where the hidden layer's output at step k-1 becomes extra input for each subsequent step k. Another memory element is introduced, combined with feedback from prior step, enhancing network's ability to grasp the system's dynamic behavior. Weights are adjusted via back-propagation during training. RNN is employed to segregate harmonic components $\mathrm{i_h}$ from load current $\mathrm{i_L}$ yielding an expression:

$$\mathrm{i_h} = \mathrm{i_L} - \mathrm{i_{base}} \tag{33}$$

In Equation (32), the fundamental component is denoted as $\mathrm{i_{base}}$ and it's crucial to highlight that reference current $\mathrm{i_{sd}^*}$ is generated by RNN, shown in Figure 6 leading to harmonic elimination. RNN comprises multiple successive recurrent layers designed to map sequences. It excels at extracting contextual information from sequences, making sequence length inconsequential when utilizing RNN. This configuration establishes a one-to-one relationship between input and output time steps, controlled by input and overlook gates regulating current input and prior hidden state.

In proposed work, HCC compare the generated reference current with actual current produced by inverter. If the actual current falls outside hysteresis band, the controller adjusts the system to bring it back within specified range. This method provides a simple and effective means of maintaining a controlled parameter within desired bounds, enhancing stability and performance in the photovoltaic system's grid integration.

VIII. RESULTS AND DISCUSSIONS

This section presents the MATLAB simulation results for proposed machine learning based PV-Grid system employing Modified Zeta-Cuk converter. Design specifications for the system are outlined in Table 1. The simulation outcomes showcase the converter's enhanced power conversion efficiency and lowered Total Harmonic Distortion (THD). Additionally, the section addresses the performance of grid-tied system concerning grid synchronization and stable operation.

The illustrations for waveforms of temperature and irradiance of solar panel is depicted in Figure 7(a) and (b). An initial temperature level of 25°C is sustained till 0.25s, after a step rise occurs and reaches the temperature level of 35°C, which is further maintained constant. In correspondence with temperature, the irradiation level of solar panel at startup stage is 800W/sq-m until 0.25s, after, the rise in temperature causes variations and results in irradiance value of 1000W/sq-m.

In Figure 8(a) the input voltage waveform is depicted, illustrating that, at the beginning stage, a stabilized voltage of 60V is maintained till 0.25s, after in response to rise in irradiance

TABLE 1. Design specification parameters.

Design Parameters	Specifications
PV System	
Peak Power	100W
Open Circuit Current	22.68V
Short Circuit Current	5.86A
Cell linked in Series	36
Modified Zeta-Cuk Converter	
L_1, L_2	1mH
C_1	4.7μF
C_0	2200μF
Switching Frequency	10kHz

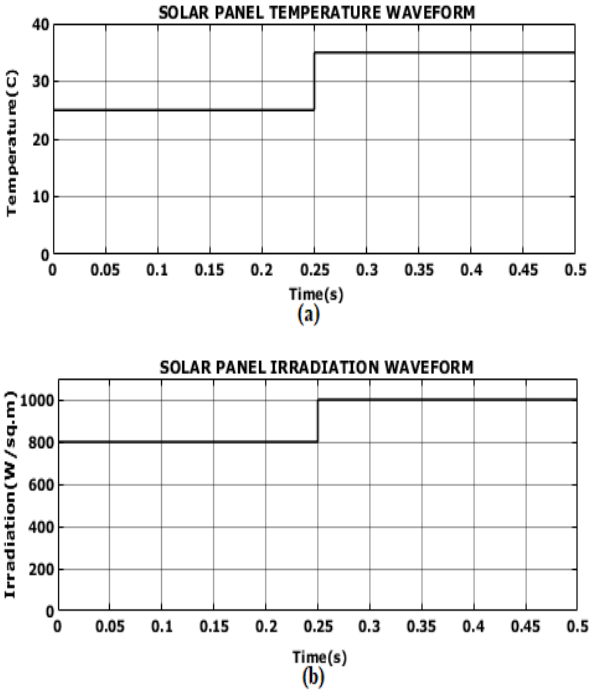

FIGURE 7. Waveform of solar panel (a) Temperature and (b) Irradiance.

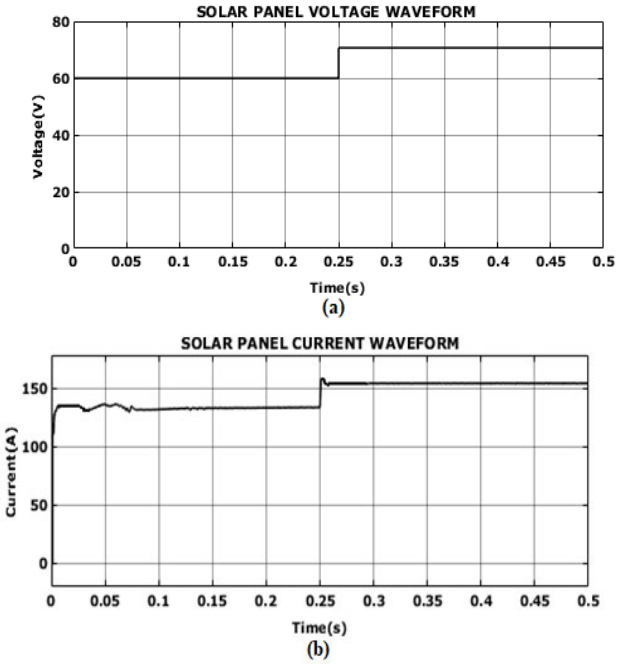

FIGURE 8. Solar panel parameters (a) Voltage and (b) Current.

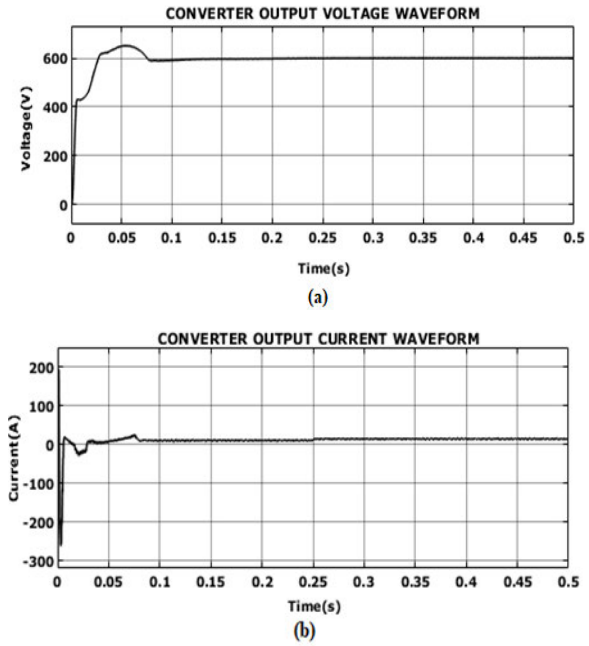

FIGURE 9. Modified zeta-cuk converter output with InC-BOA MPPT technique (a) Voltage and (b) Current.

level the voltage gets rises and attains a constant value of 70V further. In accordance with input voltage Figure 8(b) demonstrated the solar panel current waveform. From figure, it is noticed that, at the beginning fluctuation arises, with rise and fall in current level. After 0.25s, the current increases and a consistent current level of 155A is attained. The attained voltage and current is fed as input to Modified Zeta-Cuk converter.

The output voltage and current from proposed converter is depicted in Figure 9(a) and 9(b). The converter output response shows initial rise in voltage with distortions. After 0.1s, with the assistance of InC-BOA MPPT controller, a stabilized voltage of 600V is achieved without any further oscillations. Likewise, the converter current illustrated minor fluctuations at the beginning. Subsequently at 0.25s, a dependable current level of 10A is sustained further.

The response of 3Φ grid in terms of voltage and current is illustrated in Figure 10(a) and 10(b). It is noticed that, a stabilized grid voltage of 430V is accomplished using the proposed system. Subsequently, a consistent current value of 12A is achieved. This indicates that the proposed system results in optimal grid performance.

The response waveform for grid illustrating voltage and current is depicted in Figure 11. From figure, it is noticed that a stabilized voltage of 430V together with current of 12A is

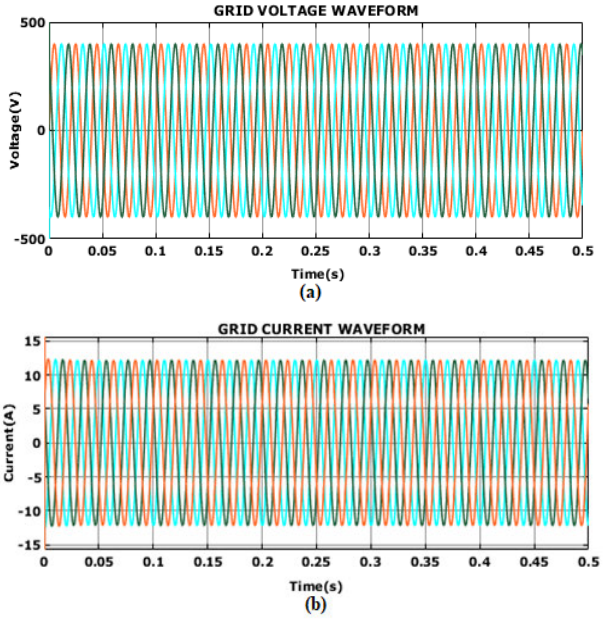

FIGURE 10. Waveforms of 3Φ grid (a) Voltage and (b) Current.

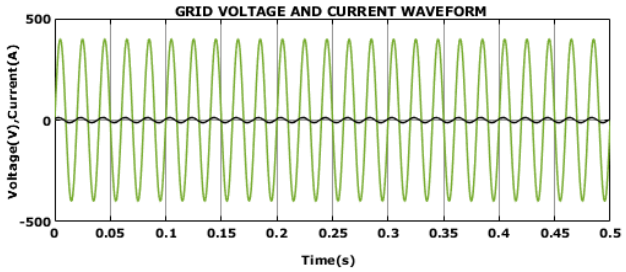

FIGURE 11. Inphase grid waveform.

accomplished. The waveform demonstrates successful management of power supply, maintaining the desired electrical parameters within the specified limits, crucial for stable and efficient operation.

In Figure 12(a) Real power waveform represents actual power transferred in a circuit, while Figure 12(b) illustrates the reactive power waveform signifying power oscillations between sources and loads. This determines the apparent power, impacting energy efficiency and system stability.

The reference current generated with the support of RNN controller is for 3Φ grid is illustrated in Figure 13. It is observed optimal reference current is produced on all the three phases using RNN controller with its sequential learning ability. By analyzing past data, the RNN predicts future current patterns, aiding in grid synchronization and enhancing control precision for power systems.

The grid current THD of 2.11%, is achieved by the proposed system, as depicted in Figure 14. This waveform shows minimal distortion in its frequency components, indicating a clean and efficient distribution of power while maintaining high-quality electrical output.

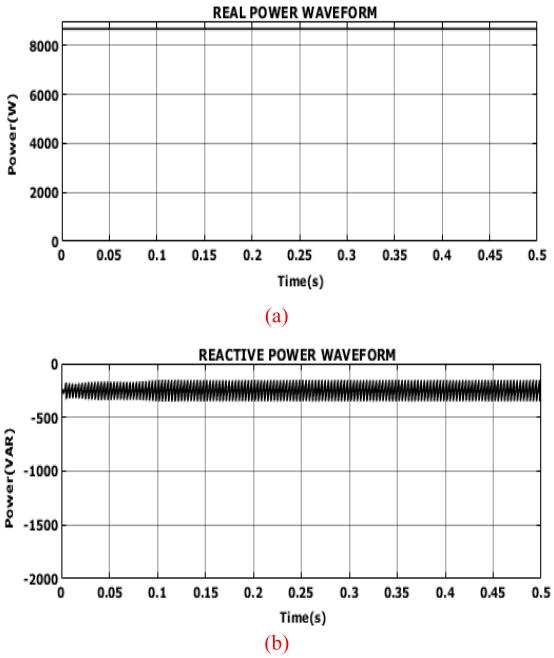

FIGURE 12. Real (P) and reactive (Q) power waveform.

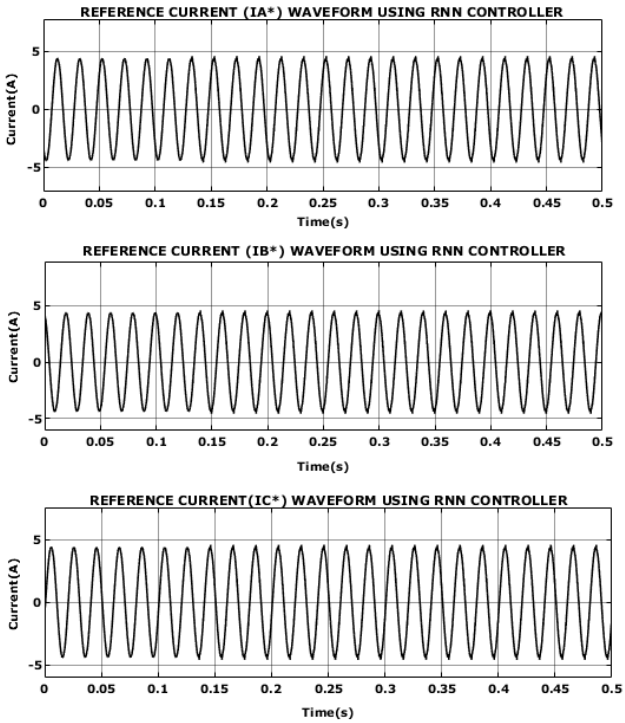

FIGURE 13. Reference current waveform using RNN controller.

Hardware Analysis:

The hardware setup of proposed framework is employed for validation purpose is illustrated in Figure 15. The laboratory prototype features a SPARTAN 6E FPGA (Field-Programmable Gate Array) functioning as a configurable

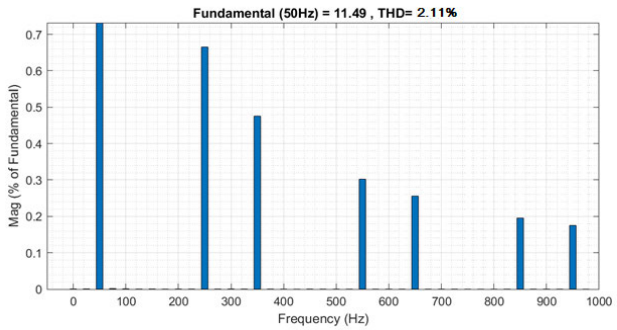

FIGURE 14. Grid current THD waveform.

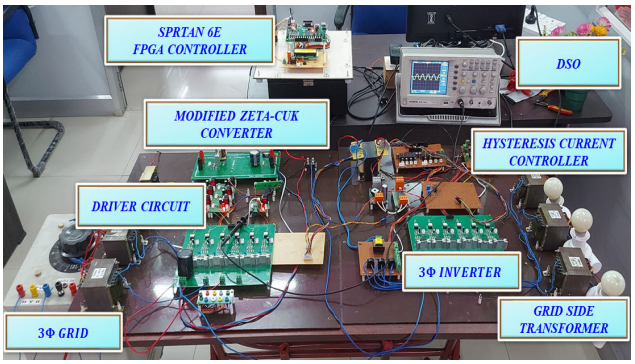

FIGURE 15. Experimental prototype.

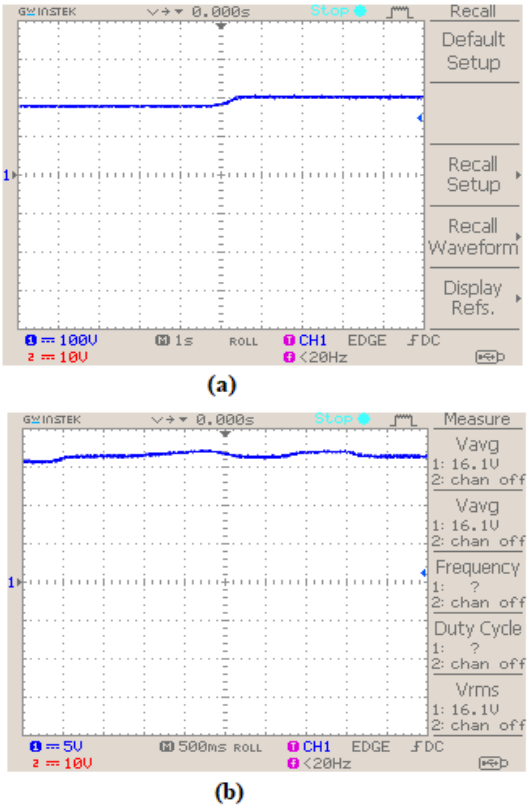

FIGURE 16. PV panel (a) Input voltage and (b) Input current waveform.

hardware controller, programmed with InC-BOA. A Modified Zeta-Cuk converter is integrated into prototype to effectively amplify the input voltage level. The presence of a driver circuit in prototype guarantees seamless incorporation and coordinated functioning of diverse components.

The voltage waveform of PV system initially displays slight distortions during the initial stage and subsequently stabilizes at 180V, as illustrated in Figure 16(a). Following this, Figure 16(b) portrays an oscillating current waveform. Eventually, a consistent PV current of 17A is attained, leading to a seamless and steady output.

In Figure 17(a), the output voltage of converter demonstrates a consistent voltage of 600V, due to the utilization of InC-BOA. Simultaneously, Figure 17(b) depicts fluctuations in the current waveform during the startup phase, followed by stabilization at a steady value later. To ensure a consistent output, enhancements might be necessary to mitigate the voltage oscillations and guarantee a dependable performance.

The waveforms in Figure 21(a) and 21(b) portray the voltage and current outcomes of 3Φ grid. A stabilized voltage and current is obtained as the results of proposed converter and control strategy. Within the context of proposed system scenarios, the introduction of an LC Filter effectively reduces the impact of harmonics generated by nonlinear loads.

The grid current waveform portrays the alternating flow of electricity in system. Notably, its low THD of 3.65% underscores the waveform's closeness to its fundamental frequency, signifying efficient power distribution with minimal distortion from harmonic influences. This attests to the grid's stable performance and adherence to quality power standards.

TABLE 2. Converter efficiency comparison.

Converter	Efficiency (%)
Modified SEPIC [28]	89.74
Modified Cuk [29]	91
Modified Luo [30]	91.5
Modified Landsman [31]	93.2
Proposed Modified Zeta-Cuk Converter	98.2

The performance of converter in terms of efficiency is contrasted with other similar modified converter topologies including modified SEPIC [28], modified Cuk [29], Modified Luo [30] and Modified Landsman [31]. It is noticed that, efficiency values of 89.74%, 91%, 91.5% and 93.2% is achieved using existing modified topologies, while the proposed Modified Zeta-Cuk converter ranks with maximum efficiency value of 98.2%, which is comparatively higher.

TABLE 3. Tracking efficiency comparison.

MPPT Techniques	Tracking Efficiency
Hill Climbing [32]	86.4%
Variable Step P&O [33]	90.5%
Variable-Step InC [34]	96%
Fuzzy [35]	97.79%
Proposed InC-BOA	98.54%

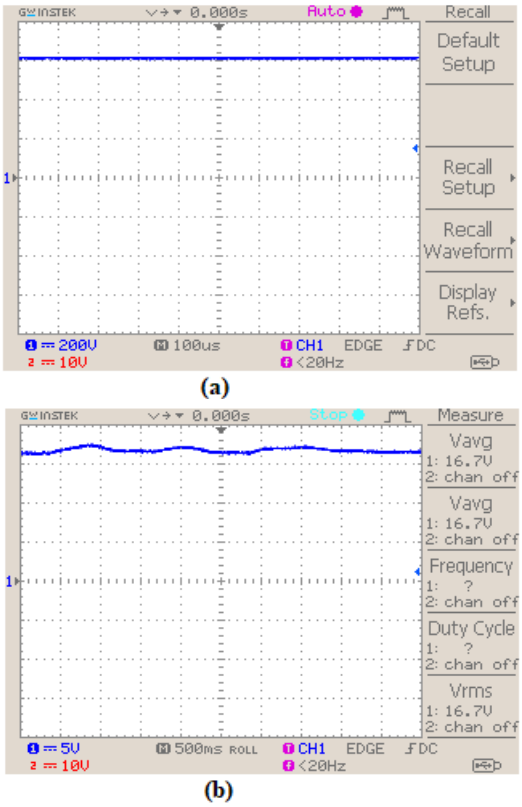

FIGURE 17. Converter waveforms (a) Output voltage and (b) Output current.

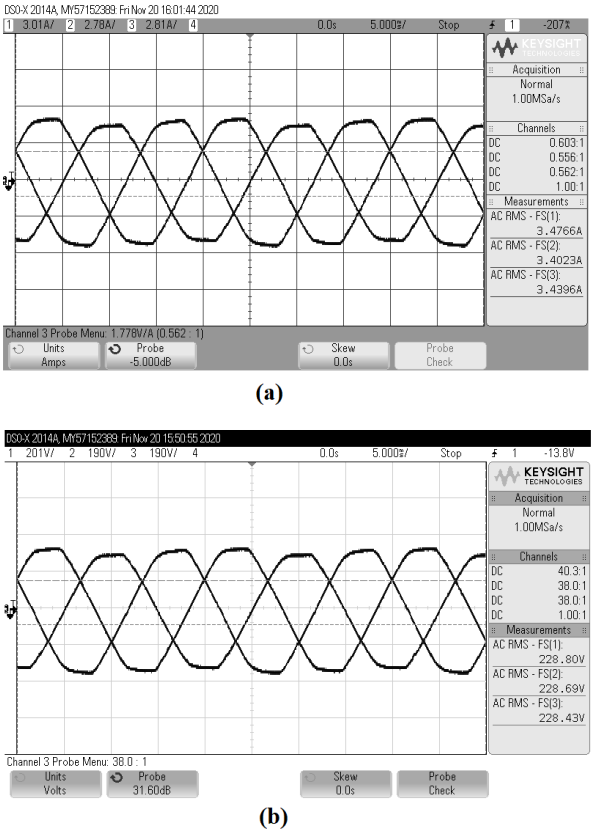

FIGURE 18. 3Φ grid (a) Voltage and (b) Current waveform.

The proposed work establishes a novel MPPT controller combined InC algorithm and BOA. To determine the analysis of proposed tracking technique approaches like Hill Climbing [32], Variable Step P&O [33], Variable Step InC [34], and Fuzzy [35] are compared and listed in Table 3. From analysis it is concluded that, proposed hybrid MPPT approach results in providing maximum efficiency value of 98.54%, which is higher in comparison with other MPPT approached stated.

The graphical representation of converter and MPPT controller efficiency is depicted in Figure 20. It is evident from the observation, that Modified Zeta-Cuk converter achieves the highest efficiency of 98.2%, whereas the tracking efficiency of InC-BOA MPPT controller attains 98.54%. In the proposed work, both converter and controller attains maximum efficiency and results in accomplishing uninterrupted optimal grid performance.

The converter output response utilizing MPPT controller like P&O, Fuzzy and proposed InC-BOA is contrasted and resulted in Figure 21. It is observed that the proposed InC-BOA MPPT controller results is maximum efficiency of 600V, at 0.1s, which is comparatively better than other controllers mentioned.

The analysis of proposed InC-BOA MPPT controller is contrasted with FLC and P&O MPPT techniques in terms of maximum output power, shown in Figure 22. It is noticed that,

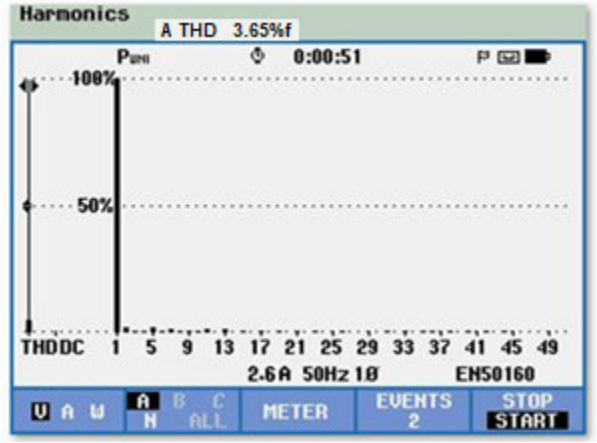

FIGURE 19. Grid current THD waveform.

minimized output power is attained using P&O technique, while FLC shows improvement than P&O approach. Meanwhile, the proposed hybrid approach combing InC and BOA results in generating maximum output power of 6kW (6000W) at irradiance level of 1000W/m^2, which is comparatively higher than other similar approach.

In a waveform depicting IAE (Integral of Absolute Error) against iteration count, the InC-BOA MPPT demonstrates its superiority in contrast to FLC and P&O technique.

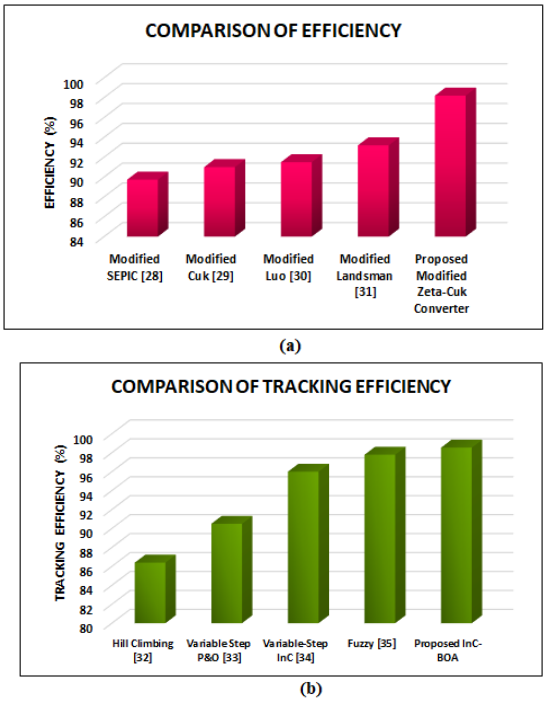

FIGURE 20. Efficiency comparison of (a) Converter and (b) Controller.

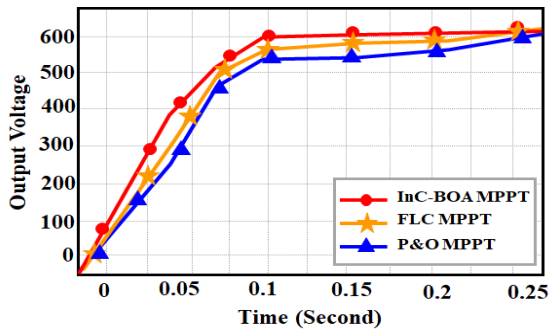

FIGURE 21. Output voltage comparison with MPPT controllers.

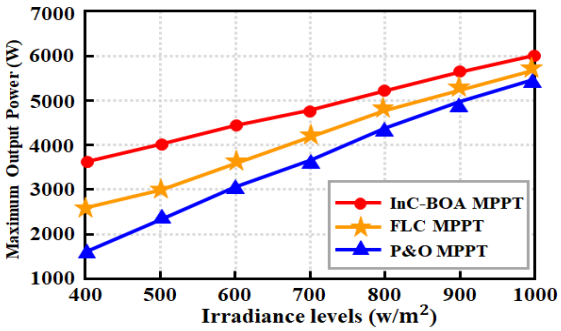

FIGURE 22. Comparison of output power vs. Irradiance.

As iterations progress, the IAE values consistently decrease, indicating a gradual reduction in the cumulative absolute error between predicted and actual values, which is evident

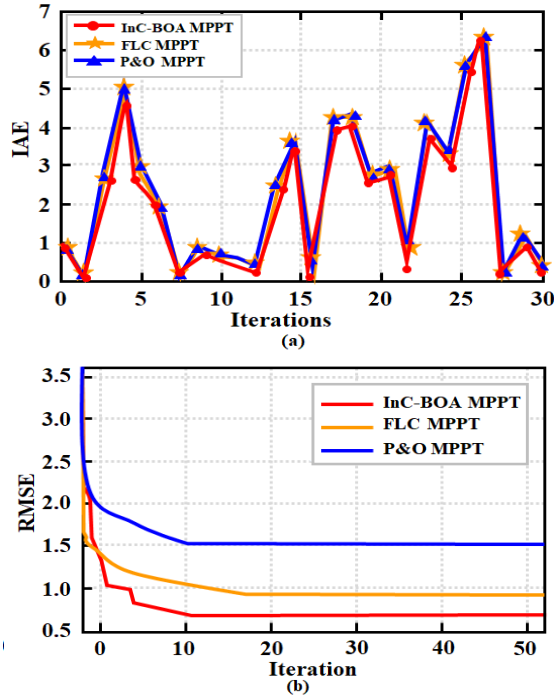

FIGURE 23. Error comparison (a) IAE and (b) RMSE.

from Figure 23(a). In contrast, the RMSE (Root Mean Square Error) of InC-BOA MPPT achieves exceptional performance, shown in Figure 23(b). This trend underscores the algorithm's ability to converge towards the true maximum power point of the solar panel, showcasing its proficiency in accurate tracking and optimization over iterations.

TABLE 4. Experimental results: THD comparison of converter.

Converter	THD
Modified Landsman [31]	4.3%
Modified SEPIC [28]	4.08%
Modified Luo [30]	3.3%
Proposed Modified Zeta-Cuk	2.11%

The performance of proposed system using Modified Zeta-Cuk in achieving grid synchronization is contrasted with respect to grid current THD and is listed in Table 4, for different converters. It is observed that, maximum THD value of 4.3% is accomplished using Modified Landsman converter of [31], while modified topologies of SEPIC [28], Luo [30] results in THD of 4.08% and 3.3%, respectively. In accordance with this, the proposed Modified Zeta-Cuk converter grades with reduced THD of 2.11%, which is comparatively lower with optimal grid performance.

The graphical representation of converter THD analysis is illustrated in Figure 24. The THD analysis is contrasted with Modified converters of Landsman [31], SEPIC [28] and Luo [30] with proposed modified Zeta-Cuk converter, of which the proposed converter ranks better with minimal THD of 2.11%. This means that the signal it generates has

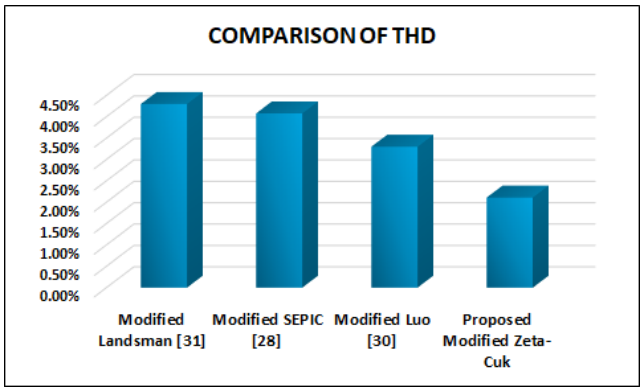

FIGURE 24. Current THD comparison.

the least amount of unwanted distortion compared to the other converters, making it a promising choice for various applications.

IX. CONCLUSION

This paper presents a pioneering approach that merges advanced control strategies and machine learning techniques to optimize the efficiency and stability of grid-tied PV systems. The Modified Zeta-Cuk converter together with InC-BOA MPPT algorithm, the voltage output of PV systems is enhanced, leading to an increased energy yield. Signal analysis, utilizing DWT and PCA, enables precise current analysis and extraction of relevant features. The integration of RNN classification model refines current control, resulting in a more accurate and stable reference current. Through MATLAB Simulink, the proposed approach showcases substantial enhancements in energy output and synchronization performance. The proposed Modified Zeta-Cuk converter achieves maximum voltage gain and efficiency of 98.2%, with InC-BOA MPPT controller accomplishing a tracking efficiency of 98.54% respectively. Also, the proposed converter results in reduced THD of 2.11%, causing grid to perform optimally. The proposed research not only advances the field of renewable energy generation but also contributes to the broader goal of sustainable energy integration into existing power grid infrastructure. Moreover, it paves the way for more durable and dependable renewable energy solutions in pursuance of a greener future.

ACKNOWLEDGMENT

The author from King Saud University acknowledge the financial support from the Ongoing Research Funding Program (ORF-2025-42), King Saud University, Riyadh, Saudi Arabia.

REFERENCES

[1] C. Breyer et al., "On the history and future of 100% renewable energy systems research," *IEEE Access*, vol. 10, pp. 78176–78218, 2022.
[2] P. Rajesh, F. H. Shajin, B. M. Chandra, and B. N. Kommula, "Diminishing energy consumption cost and optimal energy management of photovoltaic aided electric vehicle (PV-EV) by GFO-VITG approach," *Energy Sour., A, Recovery, Utilization, Environ. Effects*, vol. 47, no. 1, pp. 11823–11841, Jun. 2025.
[3] K. S. Kavin and P. Subha Karuvelam, "PV-based grid interactive PMBLDC electric vehicle with high gain interleaved DC–DC SEPIC converter," *IETE J. Res.*, vol. 69, no. 7, pp. 4791–4805, Sep. 2023.
[4] B. N. Kommula, "Efficient energy management of hybrid renewable energy sources–based smart–grid system using a hybrid IDEA–CFA technique," *Int. Trans. Electr. Energy Syst.*, vol. 31, no. 5, May 2021, Art. no. e12833.
[5] P. R. Bana, K. P. Panda, S. Padmanaban, L. Mihet-Popa, G. Panda, and J. Wu, "Closed-loop control and performance evaluation of reduced part count multilevel inverter interfacing grid-connected PV system," *IEEE Access*, vol. 8, pp. 75691–75701, 2020.
[6] B. Guo, M. Su, Y. Sun, H. Wang, H. Dan, Z. Tang, and B. Cheng, "A robust second-order sliding mode control for single-phase photovoltaic grid-connected voltage source inverter," *IEEE Access*, vol. 7, pp. 53202–53212, 2019.
[7] A. A. E. Tawfiq, M. O. A. El-Raouf, M. I. Mosaad, A. F. A. Gawad, and M. A. E. Farahat, "Optimal reliability study of grid-connected PV systems using evolutionary computing techniques," *IEEE Access*, vol. 9, pp. 42125–42139, 2021.
[8] M. A. K. Magableh, A. Radwan, and Y. A. I. Mohamed, "Assessment and mitigation of dynamic instabilities in single-stage grid-connected photovoltaic systems with reduced DC-link capacitance," *IEEE Access*, vol. 9, pp. 55522–55536, 2021.
[9] F. Blaabjerg, Y. Yang, K. A. Kim, and J. Rodriguez, "Power electronics technology for large-scale renewable energy generation," *Proc. IEEE*, vol. 111, no. 4, pp. 335–355, Apr. 2023.
[10] R. Aliaga, M. Rivera, P. Wheeler, J. Muñoz, J. Rohten, F. Sebaaly, A. Villalón, and A. Trentin, "Implementation of exact linearization technique for modeling and control of DC/DC converters in rural PV microgrid application," *IEEE Access*, vol. 10, pp. 56925–56936, 2022.
[11] J. Wang, K. Sun, C. Xue, T. Liu, and Y. Li, "Multi-port DC–AC converter with differential power processing DC–DC converter and flexible power control for battery ESS integrated PV systems," *IEEE Trans. Ind. Electron.*, vol. 69, no. 5, pp. 4879–4889, May 2022.
[12] M. I. Marei, B. N. Alajmi, I. Abdelsalam, and N. A. Ahmed, "An integrated topology of three-port DC–DC converter for PV-battery power systems," *IEEE Open J. Ind. Electron. Soc.*, vol. 3, pp. 409–419, 2022.
[13] M. Veerachary and M. R. Khuntia, "Design and analysis of two-switch-based enhanced gain buck–boost converters," *IEEE Trans. Ind. Electron.*, vol. 69, no. 4, pp. 3577–3587, Apr. 2022.
[14] R. Kushwaha and B. Singh, "Interleaved landsman converter fed EV battery charger with power factor correction," *IEEE Trans. Ind. Appl.*, vol. 56, no. 4, pp. 4179–4192, Jul. 2020.
[15] T. Sutikno, R. A. Aprilianto, N. R. Nik Idris, and A. S. Samosir, "Performance numerical evaluation of modified single-ended primary-inductor converter for photovoltaic systems," *Int. J. Electr. Comput. Eng.*, vol. 13, no. 4, pp. 3720–3732, Aug. 2023.
[16] B. Xu, Z. Yan, W. Zhou, L. Zhang, H. Yang, Y. Liu, and L. Liu, "A bidirectional integrated equalizer based on the sepic–zeta converter for hybrid energy storage system," *IEEE Trans. Power Electron.*, vol. 37, no. 10, pp. 12659–12668, Oct. 2022.
[17] X. Zhang, D. Gamage, B. Wang, and A. Ukil, "Hybrid maximum power point tracking method based on iterative learning control and perturb & observe method," *IEEE Trans. Sustain. Energy*, vol. 12, no. 1, pp. 659–670, Jan. 2021.
[18] A. K. Gupta, R. K. Pachauri, T. Maity, Y. K. Chauhan, O. P. Mahela, B. Khan, and P. K. Gupta, "Effect of various incremental conductance MPPT methods on the charging of battery load feed by solar panel," *IEEE Access*, vol. 9, pp. 90977–90988, 2021.
[19] M. Carandell, A. S. Holmes, D. M. Toma, J. del Río, and M. Gasulla, "Effect of the sampling parameters in FOCV-MPPT circuits for fast-varying EH sources," *IEEE Trans. Power Electron.*, vol. 38, no. 2, pp. 2695–2708, Feb. 2023.
[20] B. Sabir, S.-D. Lu, H.-D. Liu, C.-H. Lin, A. Sarwar, and L.-Y. Huang, "A novel isolated intelligent adjustable buck-boost converter with Hill climbing MPPT algorithm for solar power systems," *Processes*, vol. 11, no. 4, p. 1010, Mar. 2023.
[21] S. R. Kiran, C. H. H. Basha, V. P. Singh, C. Dhanamjayulu, B. R. Prusty, and B. Khan, "Reduced simulative performance analysis of variable step size ANN based MPPT techniques for partially shaded solar PV systems," *IEEE Access*, vol. 10, pp. 48875–48889, 2022.
[22] M. N. Ali, K. Mahmoud, M. Lehtonen, and M. M. F. Darwish, "An efficient fuzzy-logic based variable-step incremental conductance MPPT method for grid-connected PV systems," *IEEE Access*, vol. 9, pp. 26420–26430, 2021.

[23] S. A. Ibrahim, A. Nasr, and M. A. Enany, "Maximum power point tracking using ANFIS for a reconfigurable PV-based battery charger under non-uniform operating conditions," *IEEE Access*, vol. 9, pp. 114457–114467, 2021.
[24] C. H. H. Basha, V. Bansal, C. Rani, R. M. Brisilla, and S. Odofin, "Development of cuckoo search MPPT algorithm for partially shaded solar PV SEPIC converter," in *Soft Computing for Problem Solving: SocProS 2018*. Singapore: Springer, 2020, pp. 727–736.
[25] M. H. Ibrahim, S. P. Ang, M. N. Dani, M. I. Rahman, R. Petra, and S. M. Sulthan, "Optimizing step-size of perturb & observe and incremental conductance MPPT techniques using PSO for grid-tied PV system," *IEEE Access*, vol. 11, pp. 13079–13090, 2023.
[26] P. Lertwanitrot and A. Ngaopitakkul, "Discriminating between capacitor bank faults and external faults for an unbalanced current protection relay using DWT," *IEEE Access*, vol. 8, pp. 180022–180044, 2020.
[27] M. Hajji, M.-F. Harkat, A. Kouadri, K. Abodayeh, M. Mansouri, H. Nounou, and M. Nounou, "Multivariate feature extraction based supervised machine learning for fault detection and diagnosis in photovoltaic systems," *Eur. J. Control*, vol. 59, pp. 313–321, May 2021.
[28] A. Shawky, T. Takeshita, and M. A. Sayed, "Single-stage three-phase grid-tied isolated SEPIC-based differential inverter with improved control and selective harmonic compensation," *IEEE Access*, vol. 8, pp. 147407–147421, 2020.
[29] P. K. Maroti, M. S. Bhaskar, S. Padmanaban, J. B. Holm-Nielsen, T. Sutikno, and A. Iqbal, "A new multilevel member of modified CUK converter family for renewable energy applications," in *Proc. IEEE Conf. Energy Convers. (CENCON)*, Oct. 2019, pp. 224–229.
[30] R. Kushwaha and B. Singh, "A modified luo converter-based electric vehicle battery charger with power quality improvement," *IEEE Trans. Transport. Electrific.*, vol. 5, no. 4, pp. 1087–1096, Dec. 2019.
[31] R. Kushwaha and B. Singh, "Power factor improvement in modified bridgeless landsman converter fed EV battery charger," *IEEE Trans. Veh. Technol.*, vol. 68, no. 4, pp. 3325–3336, Apr. 2019.
[32] X. Liu and E. Sánchez-Sinencio, "An 86% efficiency 12 μW self-sustaining PV energy harvesting system with hysteresis regulation and time-domain MPPT for IoT smart nodes," *IEEE J. Solid-State Circuits*, vol. 50, no. 6, pp. 1424–1437, Jun. 2015.
[33] H. Ramadan, A.-R. Youssef, H. H. H. Mousa, and E. E. M. Mohamed, "An efficient variable-step P&O maximum power point tracking technique for grid-connected wind energy conversion system," *Social Netw. Appl. Sci.*, vol. 1, no. 12, pp. 1–15, Dec. 2019.
[34] N. E. Zakzouk, M. A. Elsaharty, A. K. Abdelsalam, A. A. Helal, and B. W. Williams, "Improved performance low-cost incremental conductance PV MPPT technique," *IET Renew. Power Gener.*, vol. 10, no. 4, pp. 561–574, Apr. 2016.
[35] D. N. Luta and A. K. Raji, "Fuzzy rule-based and particle swarm optimisation MPPT techniques for a fuel cell stack," *Energies*, vol. 12, no. 5, p. 936, Mar. 2019.

VENKATA REDDY KOTA (Senior Member, IEEE) received the Ph.D. degree in electrical engineering with Jawaharlal Nehru Technological University, Kakinada (JNTUK), Andhra Pradesh, India, in 2012. He is currently a Professor with the Department of Electrical and Electronics Engineering, JNTUK. His research interests include special electrical machines, electric drives, facts, and custom power devises and power quality. He is a member of the Institution of Engineers, India, and Indian Society for Technical Education. He was a recipient of the "Tata Rao Prize" from the Institution of Engineers, in 2012. He was also a recipient of the "IEI Young Engineers Award" from the Institution of Engineers, in 2013.

BAPAYYA NAIDU KOMMULA (Member, IEEE) received the Ph.D. degree in electrical engineering with JNTUK, Kakinada, Andhra Pradesh, India, in 2019. He is currently an Associate Professor with the Department of Electrical and Electronics Engineering, Aditya University, Surampalem. He has published around 28 papers in International journals and International Conferences. His research interests include electric vehicles, electrical drives, multilevel inverters, and renewable energy sources. He is an Active Member of IAENG.

ASIF AFZAL (Member, IEEE) received the Ph.D. degree from Visvesvaraya Technological University, in 2020. He is currently a Postdoctoral Researcher with the University of Luxembourg, specializing in computational fluid dynamics, heat transfer, machine learning, parallel computing, and optimization. He has authored or co-authored over 250 peer-reviewed publications, including works on CFD simulations, optimization techniques, and machine learning applications in engineering.

MOHAMMAD ASIF (Member, IEEE) received the Ph.D. degree from the University of Calgary, Canada, in 1991. He is currently a Professor with the Department of Chemical Engineering, King Saud University, Riyadh, Saudi Arabia. His primary research interests include carbon capture, wastewater treatment, and the application of fine and ultrafine particle technology in separation and reaction systems.

LIEW TZE HUI (Member, IEEE) received the Bachelor of Project Management (B.P.M.) and Master of Science (M.Sc.) degrees from Universiti Utara Malaysia, and the Ph.D. degree in information technology from Multimedia University (MMU), Malaysia. He is currently a Senior Lecturer with the Faculty of Information Science and Technology (FIST), MMU, Melaka campus.